Ventilation for Energy Efficiency and Optimum Indoor Air Quality
13th AIVC Conference, Nice, France
15-18 September 1992

Paper 21

Contaminant Dispersal Measurement Using Laser Light Sheet Illumination and Digital Image Processing Techniques.

J.W. Axley and L.K. Norford

Building Technology Program, Massachusetts Institute of Technology, 77 Massachusetts Avenue, Cambridge, MA 02139, USA.

Synopsis

This paper describes a method for measuring the dispersal of airborne contaminants by light-sheet illumination of aerosol tracers and digital image processing techniques. The goals of the research were two-fold: to use field-portable and safe equipment to make near-instantaneous measurements of tracer aerosol concentrations over arbitrarily positioned two-dimensional planes of near-room dimensions; and to carefully define similarity conditions under which aerosol dispersal can be considered an accurate surrogate for passive molecular dispersal.

The measurement method involves five procedures: tracer generation by condensation of a glycol vapor; light sheet illumination using a projected laser; image capture using a CCD video camera linked to an analog-to-digital converter; point-calibration measurement, via light attenuation, of aerosol concentration; and image processing using a public-domain microcomputer-based program. This paper will briefly review the method and evaluation tests and will emphasize technical and theoretical issues concerning the relationship between captured images and aerosol concentration and the similarity of tracer to molecular dispersal.

List of Symbols

C is the molecular species concentration, moles/m^3.

$\overline{C}$ is the time-smoothed concentration averaged across the section of the duct.

c_f is a friction coefficient.

$\vec{c}$ is the particle migration velocity vector (e.g., settling velocity), m/s.

D is a characteristic dimension of the flow regime, m.

$\mathcal{D}_\alpha$ is the molecular diffusivity of a species α, m^2/s.

$\mathcal{D}_p$ is the particle diffusivity of the aerosol particles, m^2/s.

$\vec{f}$ is a rapidly varying stochastic force due to molecular agitation, g-m/s^2.

I is the intensity of light, lumens/m^2 or watts/m^2

m is the effective mass of the particle, g

n is the particle concentration, #/m^3.

n^* is a dimensionless concentration equal to the concentration divided by a reference concentration.

R is the radius of the duct, m.

r_t is the radius of the particle, μm

r_t/D is the interception parameter.

$Re \equiv DV/\nu$ is the Reynolds number.

$Sc_p \equiv \nu/\mathcal{D}_p$ is the aerosol particle Schmidt number.

$Sc_\alpha \equiv \nu/\mathcal{D}_\alpha$ is the molecular Schmidt number for species α.

t^* is a dimensionless time equal to $(V\,t/\mathcal{D}_p)$ or $(V\,t/\mathcal{D}_\alpha)$.

$\vec{u}$ is the particle velocity, m/s.

$\vec{v}$ is the local fluid velocity vector , m/s.

$\vec{v}^*$ is a dimensionless velocity equal to the actual velocity divided by a suitable reference velocity V.

$\overline{v}$ is the time-smoothed mean velocity.

x is the distance along a duct, m.

z is the distance along a given optical path, m

γ is the extinction coefficient, m^{-1}

$\nabla^* \equiv D\,\nabla$ is a dimensionless del operator, where D is a suitable reference dimension.

ν is the kinematic viscosity of the fluid (e.g., air), m^2/s.

1. Introduction

The growing concern for the quality of air in indoor environments and the economic importance of air contaminant control in clean room design have together focused attention on contaminant dispersal in buildings, in general, and within room in particular. Actual personal exposure to indoor air pollutants [1] and the success or failure of a clean room design both depend critically on the spatial distribution, or mixing, of

contaminants within rooms and the variation of this mixing with time.

Recognizing the critical importance of mixing, researchers in the field have attempted to study the general character of room mixing using both experimental and computational techniques. Airborne contaminant distributions in rooms have been measured using discrete, point-sampling techniques. These techniques, however, (a) provide poor spatial and temporal resolution, (b) tend to be invasive, and (c) tend to be limited to laboratory investigations due to their complexity and expense.

Computational determination of velocity flow fields and the associated computational determination of tracer dispersal driven by these flow fields – *microscopic analysis* – offers a very attractive alternative to the experimental approach because, in principle, the dispersal in space and time may be determined to any degree of resolution [2-5]. Regrettably, however, this analysis must be based on semi-empirical *dispersal turbulence models* that have yet to be thoroughly validated and is presently limited to rooms of simple geometry and stationary flow conditions.

On the one hand, then, experimental evaluation of mixing based on discrete sampling can not provide sufficient data to fully characterize the spatial or temporal nature of mixing in rooms and, on the other, computational determination of dispersal can not be considered reliable until experimental techniques are developed that can provide the detail needed for their validation. Laser light sheet illumination techniques have the potential to provide an answer to this dilemma.

Building on light slit illumination techniques, several investigators have illuminated reflective aerosol tracers in various flow fields by laser light sheets to effectively reveal the qualitative structure of the flow field and its variation with time [6, 7]. Saunders and Albright described the preliminary development and feasibility testing of a method to quantitatively investigate pollutant mixing by illuminating glycol aerosol tracers and processing captured images [8]. They assumed (a) tracer concentration was proportional to scattered light intensity, (b) tracer aerosol dispersal would be similar to passive molecular dispersal, and (c) only scattered light was received by the image acquisition system. The work described in this paper addresses these assumptions explicitly in an effort to establish the limitations of quantitative measurement of sheet-illuminated aerosol tracer distributions in room airflow.

2. Development of the Proposed Method

The measurement method reported herein evolved over a two-year period through review of the literature and a series of trial and error investigations relating primarily to (a) the selection of an appropriate aerosol tracer, (b) the selection of system components from those that were commercially available, (c) the development of experimental protocol, and (d) the selection of tests that would aide in the development of the method.

2.1 Measurement Method and System Components

The measurement method investigated involves five procedures supported by the hardware and software components described below and illustrated in Figure 1.

Tracer Generation & Injection: A glycol-based condensation generator was used to generate an aerosol tracer. This *theatrical fog generator* provides an aerosol tracer that scatters light efficiently yet is harmless and what little residue it leaves can be easily cleaned. Detailed particle size distribution measurements indicate that initially the generated aerosol is practically monodisperse with a mean particle diameter of approximately 0.5 μm. It then undergoes agglomeration, the mean diameter grows with time, the particle size distribution spreads to become polydisperse, and eventually settling of the larger particles becomes significant. To allow the initial rapid agglomeration to pass before injection and to better control tracer injection, generated fog was temporarily stored in an accordion-like collapsible storage cylinder approximately 2 m by 0.3 m in diameter. Subsequent tracer injection was realized by the controlled collapse of the storage cylinder.

Light Sheet Illumination: A *dynamic light sheet*, generated by projecting a laser light beam onto a rapidly oscillating mirror (*scanner*) to scan the beam over a triangular segment of a plane, was used to illuminate the aerosol. Hardware components included a 50 mW Argon ion laser and commercially available optical components, function generator, amplifier, and scanner. The laser was selected from among the highest output power lasers that can operate on standard 120 V, 15 amp supply. This class of lasers is also relatively safe and field portable.

Image Capture & Point Measurement: Images were captured using a CCD video camera linked to a microcomputer-based analog-to-digital converter that together provided a gray level resolution of 256 values (i.e., 8 bit). A simultaneous concentration measurement was made at a single point within the field of view to allow calibration of the captured image.

Image Processing: Digital processing of the acquired images was required to correct for both systematic error (*normalization*) and random error (*noise reduction*) and to transform the recorded gray level data to tracer concentration values (*calibration*). All image processing was realized using the program Image 1.40; a public-domain program distributed through the National Institutes of Health.

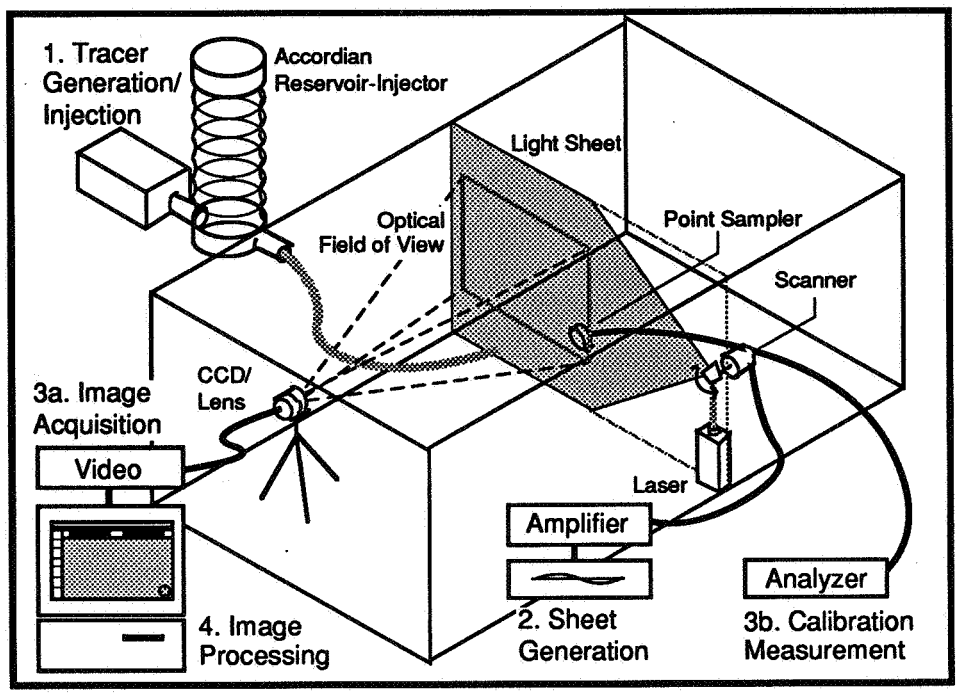

Figure 1. Laser light sheet measurement system components.

2.2 Development Test Series

The development of the method was based on tests that would allow fundamental evaluation of the spatial and temporal resolution, accuracy, and repeatability of the proposed method rather than investigating specific cases of contaminant dispersal in rooms. Four test series were central to the development of image normalization, noise reduction, calibration, and measurement protocol and used to evaluate similarity:

Aerosol Particle Size Distribution Measurements: measurements of the particle size distribution of the freshly generated aerosol and its variation with time to (a) provide data needed to develop a relation between extinction measurement and concentration used for calibration purposes, and (b) to evaluate time-dependent transformations of the aerosol tracer due to agglomeration,

No-Flow Compartment Tests: tracer dispersal studies in a small, sealed, well-mixed chamber to evaluate the reliability of proposed normalization and noise reduction procedures by comparison of measured distribution uniformity with expected uniformity and to assess time-dependent transformations of the aerosol tracer,

Steady-Flow Compartment Tests: tracer dispersal studies in a small, well-mixed chamber under conditions of steady ventilation flows to evaluate the accuracy of the method at moderate rates of data acquisition necessary to capture slowly varying concentration fields and to again evaluate the reliability of proposed normalization and noise reduction procedures, and

Stationary Flow Duct Tests: tracer dispersal studies in a 12 m long circular duct of 0.30 m diameter under stationary turbulent flow conditions to evaluate the accuracy of the method at high rates of data acquisition necessary to capture rapidly varying concentration fields.

3. Relating Scattered Light to Aerosol Concentration

If interest is limited to the dispersal of aerosols similar to the properties of the aerosol tracer used in the proposed measurement method then one need only be concerned with the ability of the image acquisition system to record scattered light from the illuminated field and the relation between recorded scattered light and tracer concentration or density.

3.1 Aerosols Properties and Behavior

The proposed method depends on the efficiency with which the chosen aerosol scatters light from the

light sheet. Broadly speaking, aerosol particles are classified into three groups: particles small relative to the wavelength of the incident light; particles very much larger than the wavelength of the incident light; and those falling in the range in-between. Rayleigh scattering theory predicts, and measurements confirm, that small-particle aerosols scatter light inefficiently; classical optical theory predicts that large-particle aerosols will scatter light more efficiently; and Mie theory predicts that the moderate-sized aerosols will scatter light most efficiently for a given volume of particles. Hence, to maximize light scattering we prefer to use aerosols with particle sizes just above the Rayleigh, small-particle range or, for visible light scattering, above the 0.1 to 0.5 μm particle diameter range.

The intensity of light scattered from a given aerosol may be increased simply by increasing the concentration of the aerosol, but there are practical limitations to this strategy. At very high concentrations the aerosol will tend to obstruct both the view of the illuminated sheet and the ability of the laser to illuminate the sheet evenly - both unacceptable conditions. At moderate concentrations an undesirable and generally unknown nonlinear relation will exist between aerosol concentration and scattered intensity, due to the increased probability of *multiple scattering*, that will complicate the calibration of captured images. Multiple scattering will create so-called *virtual emissions* within the view of the image acquisition system that will tend to veil the light scattered from the illuminated sheet.

Finally, all aerosols tend to agglomerate or suffer deposition as individual particles collide with each other or surfaces and, as a result, the size distribution and, to a lesser extent, the amount of aerosol varies with time. The time variation of particle sizes can result in a variation in scattered light intensity that is unrelated to aerosol concentration and as such must be minimized. As higher concentrations will tend to accelerate the rate at which aerosol particles agglomerate we shall prefer to implement the proposed method using low aerosol tracer concentrations.

3.2 Experimental Protocol

Considering all these factors then, we prefer to inject tracers with particle size distributions just above the Rayleigh scattering size range at concentrations sufficiently low so that the aerosol particle size distribution does not vary significantly during the test time period. Measurements of our condensation-generated glycol aerosol indicate these objectives may be achieved by generating then temporarily storing the aerosol (e.g., for 10 minutes) - to allow an initial stage of rapid agglomeration to pass - before injection. By maintaining peak aerosol concentrations within a concentration range of 10^5 to 10^7 particles/cm^3 scattered intensities remain detectable (i.e., with our equipment) yet changes due to agglomeration vary slowly with an effective time constant on the order of tens of minutes.

3.3 Image Processing

Captured images of practically uniform distributions of aerosol proved not to be uniform – they not only contained consistent unstructured nonuniformities (e.g., lighter and darker edges and "smudges") but revealed consistent structured patterns of vertical stripes from image to image. A composite of three images of light scattered from a uniformly distributed aerosol tracer is illustrated in Figure 2 with histographic distributions of gray-values shown for each third. The lower third of this image is a pseudo gray-scale representation of the raw image data. To correct for sources of systematic error, captured images were normalized against light scattered from well-mixed distributions of aerosol tracer following the example of Long et al [9, 10]. The result of this normalization is indicated by the middle third of Figure 2. (Details of the normalization algorithms will be included in a forthcoming report.)

The vertical stripes evident in the raw image due, presumably, to electromagnetic interference are visually obvious but also indicated by the bimodal character of the histograph in this case. Less obvious, but indicated by the alternating comb-like appearance of the raw data histograph, is the fact that analog-to-digital board used favored odd gray-values. Finally, a careful examination of the series of images taken during this particular test reveals consistently brighter conditions along the lower and left edges of the images.

Normalized images revealed a *salt and pepper* distribution of gray values that is characteristic of random error due to electromagnetic noise, the *dark current* produced by CCD devices, or to the natural stochastic distribution of the aerosol itself. Two standard schemes to remove this source of error were considered – *mean* and *median filtering* – wherein each pixel value of an image is replaced by the either the mean or median of the pixel values in the 3 x 3 array of pixels centered on the chosen pixel. Both strategies appeared to be equally effective, although, given the expected stochastic distribution of the aerosol particle sizes, the mean filtering should be more appropriate. The result of this noise reduction is indicated by the upper third of Figure 2.

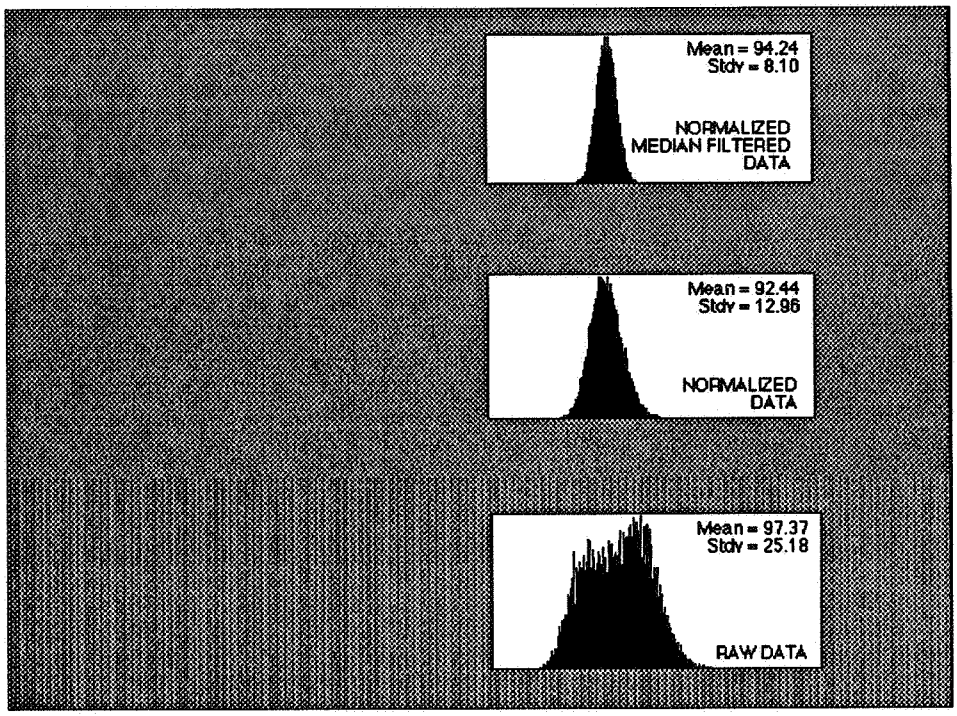

Figure 2. Representative results of normalization and noise reduction of images captured from a uniform distribution of aerosol tracer.

3.4 Calibration

The aerosol tracer concentration was calibrated by relating the intensity of scattered light at a single point in the captured image to a particle concentration estimated on the basis of a light extinction measurement. The extinction coefficient, defined as fraction of light scattered and/or absorbed within a media per unit length of optical path:

$$\gamma \equiv -\frac{dI}{Idz} \tag{1}$$

can be linearly related to the particle number concentration, using Mie scattering theory, when the number distribution of particles as a function of size is known and conditions of single, independent scattering are realized. These conditions are realized when the optical depth, the integral of the extinction coefficient over the path from the sheet to the acquisition system, is less than approximately 0.1.

4. Similarity of Aerosol and Molecular Dispersal

Strictly speaking, the dispersal of the chosen aerosol tracer may be expected to be similar only to other aerosols with the same particle size distributions and densities. Practically, however, we may identify conditions under which the aerosol dispersal will be similar to other contaminants and, specifically, to molecular species. A *first similarity condition* relates to agglomeration. By maintaining conditions of low aerosol concentrations, as discussed above, the effects of agglomeration may be mitigated.

4.1 Miscible Two-Phase Continuum Transport

To identify additional similarity conditions it is useful to compare continuum two-phase convection-diffusion transport theory for molecular and aerosol transport (e.g., see [11, 12]):

Molecular Transport
$$\frac{\partial C}{\partial t} + \vec{v} \cdot \nabla C = \mathcal{D}_\alpha \nabla^2 C \tag{2}$$

Aerosol Transport
$$\frac{\partial n}{\partial t} + \vec{v} \cdot \nabla n = \mathcal{D}_p \nabla^2 n - \nabla \cdot \vec{c} n \tag{3}$$

These two equations will have the same form if the last term of Equation 3, the settling velocity term, becomes negligible. This establishes a *second similarity condition* that particle sizes must be small enough so that settling is insignificant. Practically, this limits particles to diameters smaller than about 10 μm.

Equations 2 and 3, with the settling term removed, may be recast in dimensionless form as:

$$\frac{\partial n^*}{\partial t^*} + \vec{v}^* \cdot \nabla^* n^* = \frac{1}{Re\,Sc} \nabla^{*2} n^* \qquad (4)$$

Consequently, molecular dispersal will be similar to aerosol dispersal when the product *Re Sc* is of similar magnitude for each case; $Re\,Sc_\alpha \approx Re\,Sc_p$. For full-scale or field measurements the Reynolds numbers will be identical so we may assert a *third similarity condition* that Schmidt number similarity is needed to achieve our objective.

Regrettably, aerosol particle diffusivities, for the particle size range of use here (0.5 to 10.0 μm), are on the order 10^{-7} cm^2/s while molecular diffusivities are some six orders of magnitude larger. Kinematic viscosities for both aerosol-air and molecular-air systems will be of similar magnitude – in the range of 1 to 2 x 10^{-1} cm^2/s. Consequently, molecular Schmidt numbers may be expected to be close to 1 while particle Schmidt numbers will be near 10^6 and, as a result, it will be practically impossible to satisfy this third condition. If, however, the diffusion term of Equation 4 is negligibly small (i.e., transport is dominated by convective processes) then this third condition becomes irrelevant. For turbulent flow, this becomes the case as, from one perspective, molecular or particle diffusivities become overwhelmed by *eddy diffusivity* (i.e., due to small scale turbulence) that is expected to be (nearly) identical for both cases. (Consideration of the time-smoothed formulations of Equations 2 and 3 using the eddy diffusivity turbulence model, leads to this last conclusion.)

The *third similarity condition*, therefore, establishes two limiting conditions. At one extreme, for fully developed turbulent flow the dispersal of aerosol particles and molecular species may be expected to be practically identical as eddy diffusion will dominate. At the other extreme, for very low flow the dispersal of aerosol particles can not be expected to be similar to that of molecular species. Between these limiting cases one may encounter situations where convective, yet nonturbulent, transport dominates the flow (e.g., laminar flow in clean rooms) and thus the diffusion term becomes negligible and similarity is realized or, alternatively, where particle/molecular diffusion transport is significant and, hence, similarity can not be expected.

The particle/molecular-diffusion limit may not be critical in room studies as room air is invariably in motion due to ventilation, infiltration, and natural convection and, as a result, true stagnant conditions are practically never achieved. Rodes reviews measurements of air velocity and turbulence intensity (i.e., the relative standard deviation of velocity) in rooms that indicate average velocities on the order of 5 cm/s with HVAC systems off and 15 cm/s with HVAC systems on, with turbulence intensities ranging from 20-120% [1]. Most airflows in rooms may, therefore, be expected to exceed 2 cm/s. From kinetic theory, the net velocity of a single particle, due to Brownian motion, or a single molecule, due to kinetic motion, is on the order of $\sqrt{2\,\mathcal{D}_p}$ or $\sqrt{2\,\mathcal{D}_\alpha}$ respectively [13]. For the representative diffusivities discussed above, then, the net kinetic velocity of a single molecule will be approximately 0.3 cm/s and that of a tracer aerosol particle 0.0003 cm/s, both substantially less than expected minimum air velocities in rooms. From this discussion we may establish a *fourth similarity condition*: if minimum flow velocities are well above the net kinetic velocity of the molecular species being considered, $\sqrt{2\,\mathcal{D}_\alpha}$, then one may assume that diffusion transport mechanisms are negligible and, consequently, the dispersal of molecular and tracer particle species will be similar. Regrettably, in laminar flow situations this condition may not be satisfied in directions orthogonal to the flow streamlines.

The boundary conditions for aerosol particle transport are necessarily different from those used for molecular transport because of the finite size of aerosol particles [12]. As particles will intercept the boundary upon surface contact, one may define a boundary condition that the aerosol particle concentration becomes zero at a distance equal to the radius of the particle r_t from the surface rather than directly at the surface. As a consequence, an added dimensionless variable, the interception parameter r_t/D, may be introduced. Effectively, for molecular flow the interception parameter is zero. A *fifth similarity condition* may then be stated that aerosol particle dispersal will be similar to molecular dispersal when the interception parameter is practically negligible. That is to say, we can not expect to resolve dispersal detail approaching the tracer particle size close to surfaces. This condition presents no practical problem in room distribution measurements for the tracers used.

4.2 Non-Continuum Transport

From a microscopic point of view aerosol particles are discrete, finite objects submerged in a fluid flow field and no longer appear to be a continuous phase. As discrete, finite objects, particles will tend to lag behind fluid motion in regions of accelerating flow.

This case may be analyzed following the argument presented by Long et al. [9]. An equation of motion may be formulated for an individual particle as:

$$m\frac{d\vec{u}}{dt} = c_f(\vec{v} - \vec{u}) + \vec{f} \quad (5)$$

where it is normally assumed that $\vec{f}$ is independent of the velocities, fluctuates more rapidly than the velocities, and has a mean value that vanishes over time [12].

Equation 5 clearly indicates that particles lag behind fluid velocity – *slip* – when accelerated. Furthermore, the frictional force acting on the particle $c_f(\vec{v} - \vec{u})$ tending to correct the slip is directly related to the *slip velocity* (i.e., the relative particle velocity $(\vec{v} - \vec{u})$). Given the independence of $\vec{f}$, Equation 5 and, hence, the slip velocity may be characterized by a relaxation time constant:

$$\tau_{relax} = \frac{m}{c_f} \quad (6)$$

that provides an order-of-magnitude estimate of the time required for a particle to "catch-up" with the airflow.

Using published correlations for the friction coefficient [12] and the physical properties of the aerosol system used in the current investigation the relaxation time constant, τ_{relax}, will range from 7×10^{-5} s to 5×10^{-6} s for particle Reynolds numbers ranging from 0 to 1000. Within occupied regions of rooms airflows are normally limited for comfort reasons to approximately 0.25 m/s and, as the instantaneous slip velocity is bounded by this value, maximum particle displacement lags would be well below the spatial resolution of the proposed measuring method:

$$\tau_{relax}(\vec{v} - \vec{0}) \approx (7 \times 10^{-5}\ \text{s})(0.25\ \text{m/s}) = 17.5\ \mu m$$

Air velocities at diffusers may be as much as two orders of magnitude greater so displacement lags may conceivably approach 2000 μm or 2 mm – still within the spatial resolution of the measurement method.

From this analysis we may assert a *sixth similarity condition* that aerosol dispersal will be similar to molecular dispersal if the slip relaxation time of the particles is small. For room airflow dispersal studies the Rosco fog should satisfy this condition. That is, we should expect the lag of Rosco fog particles in regions of accelerating flow to be negligible.

4.3 Immiscible Two-Phase Continuum Transport

A sufficiently dense aerosol cloud having well-defined boundaries will tend to act, at least initially, as a single body of immiscible fluid. The motion of such a cloud will be determined not by the motion of individual particles but by the bulk mechanics of the cloud as a whole, consequently, the cloud may settle at a faster rate than individual particles in the cloud. For the present application, *cloud settling* may prove to be a problem when injecting an aerosol tracer into a flow regime under study.

Hinds provides an introductory discussion of the bulk motion of aerosols [13] although the descriptive theory presented is limited to the settling of a spherical aerosol cloud. To gain some sense of the importance of cloud settling the table below (abridged from a similar table in Hinds [13]) shows the number concentration that will result in a cloud settling velocity of 1 cm/s for various values of particle diameter and cloud diameter for particles of specific gravity 1.0 at standard conditions.

	Number Concentration (cm^{-3}) for a Cloud Settling Velocity of 1 cm/s	
Particle Diameter (μm)	Cloud Diameter = 1 cm	Cloud Diameter = 10 cm
0.1 μm	8.5×10^9	2.0×10^8
0.4 μm	1.3×10^8	3.1×10^6
1.0 μm	8.5×10^6	2.0×10^5

Table 1 Number concentration to produce a cloud settling velocity of 1 cm/s for a spherical cloud of 1 μm particles of unit specific gravity in air at standard conditions.

From this discussion we made establish a *sixth similarity condition* that aerosol tracers must be injected at sufficiently low concentrations to avoid significant cloud settling. For injection plumes on the order of centimeters or less this will limit injected tracer concentrations to values less than 10^6 to 10^8 particles/cm^3.

5. Stationary-Flow Duct Test Results

The test setup for the stationary flow duct test is illustrated below in Figure 3. In these tests aerosol

tracer was injected as a pulse upstream in a 12 m long circular duct of 0.30 m diameter under conditions of stationary turbulent flow, a plane was illuminated with the laser sheet 6 m downstream, and images of the resulting scattered light were recorded at rapid intervals as the aerosol pulse passed through the laser light sheet. These tests were devised to challenge the data acquisition rate of the system.

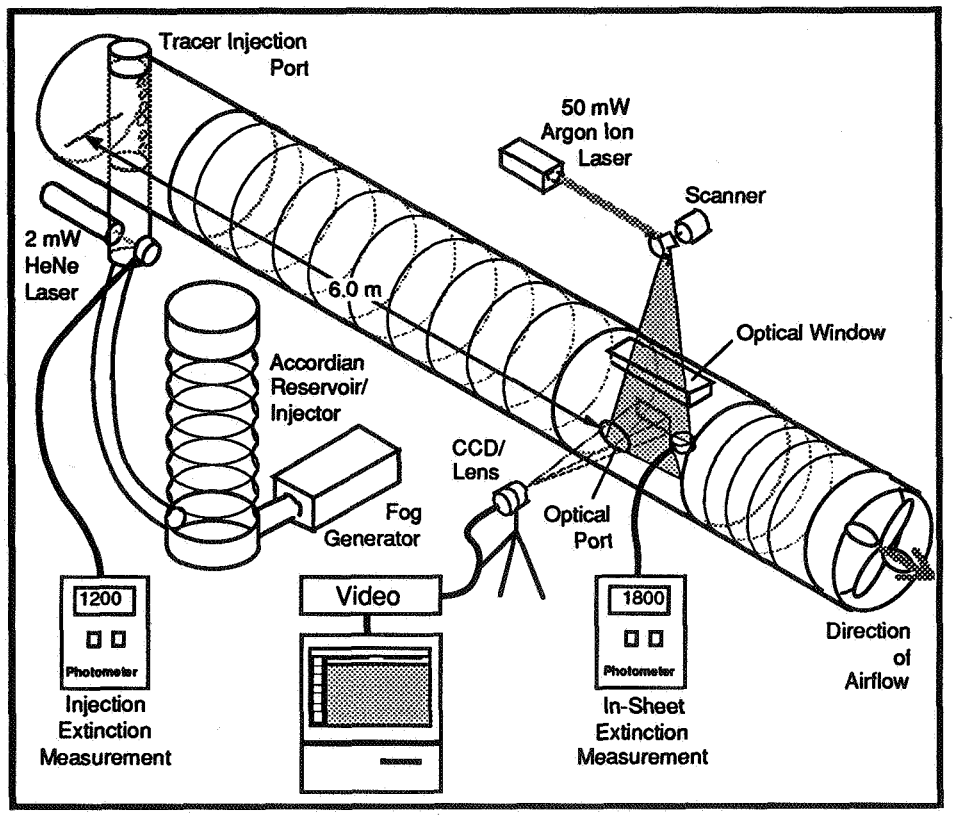

Figure 3 Configuration of the duct test systems.

Several pulse injection tests were conducted at a range of flow Reynolds numbers from 3,220 to 35,400 and measured results were compared to predicted results obtained from finite-element solutions of the 1D axial-dispersion equation:

$$\frac{\partial \overline{C}}{\partial t} + \bar{v}\frac{\partial \overline{C}}{\partial x} = \mathcal{D}_{eff}\frac{\partial^2 \overline{C}}{\partial x^2} \tag{7}$$

The *effective* or *axial* dispersal coefficient, $\mathcal{D}_{eff}$, is well correlated to the flow Reynolds number alone for fully developed turbulent flow (i.e., Re > 10,000) [14, 15]:

$$\mathcal{D}_{eff} \approx 2\bar{v}R\left(\frac{3.0\ x\ 10^7}{Re^{2.1}} + \frac{1.35}{Re^{0.125}}\right) \tag{8}$$

All predicted results were based on this equation that may be expected to yield accurate results for Re > 2,500 and Sc ≈ 1 – that is to say for molecular dispersal.

In the laminar flow regime (i.e., Re < 2,500) the nature of axial dispersion changes considerably as radial transport becomes more dependent on the diffusivity of the phase being transported. Transported phases having a high Schmidt number (low diffusivity), such as the Rosco fog, will tend to experience more rapid transport in the core flow as radial transport will be inhibited and flow velocities in the core are greater than in the perimeter. Effective dispersal coefficients are, consequently, greater in laminar flow than in fully turbulent flow (Levenspiel 1962). The nature of dispersal for phases with particularly high Schmidt numbers like the Rosco fog in the transition region (i.e., 2,500 ≤ Re ≤ 10,000) has not been well studied.

Representative comparisons of measured and predicted results are illustrated in Figures 4, 5 and 6. Each of these figures illustrates the predicted results for the estimated Reynolds number (solid line) and for Reynolds number 10% smaller and greater (gray lines), corresponding to the uncertainty in mean air flow velocity measurement. Error bars corresponding to the standard deviation of the (spatial) mean gray value of each captured image along with the mean gray value itself (solid markers) are also illustrated.

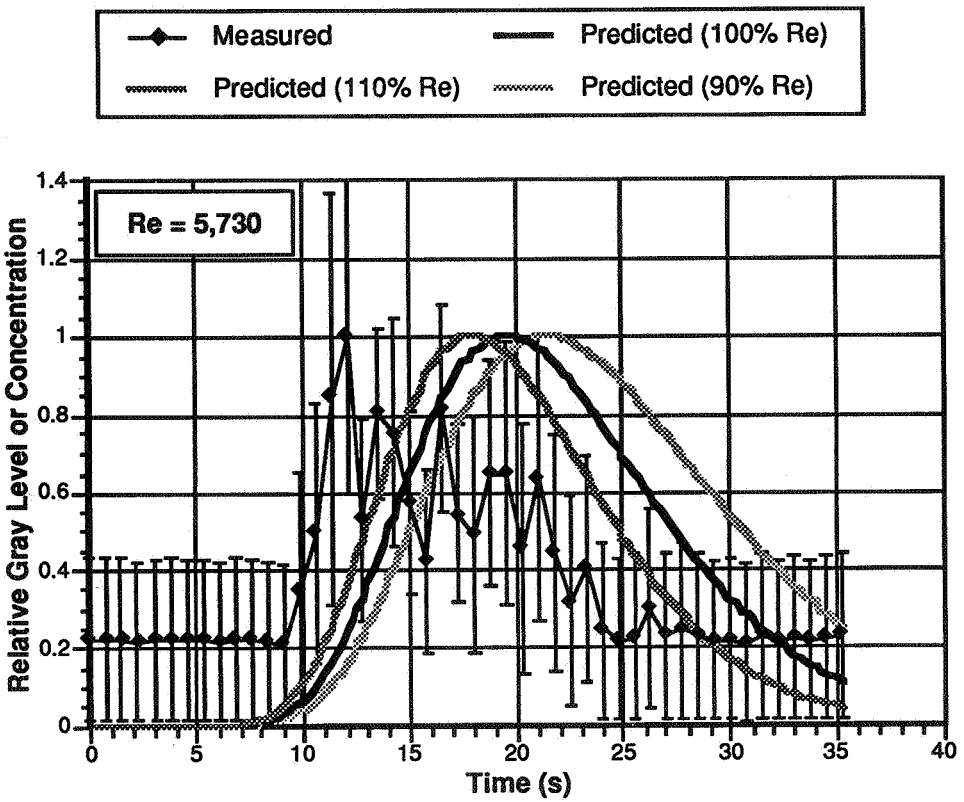

Figure 4 Comparison of measured mean gray level and predicted aerosol concentration time histories of a passing tracer pulse in a 0.30m diameter duct under conditions of transitional flow with a Reynolds number of 5,730.

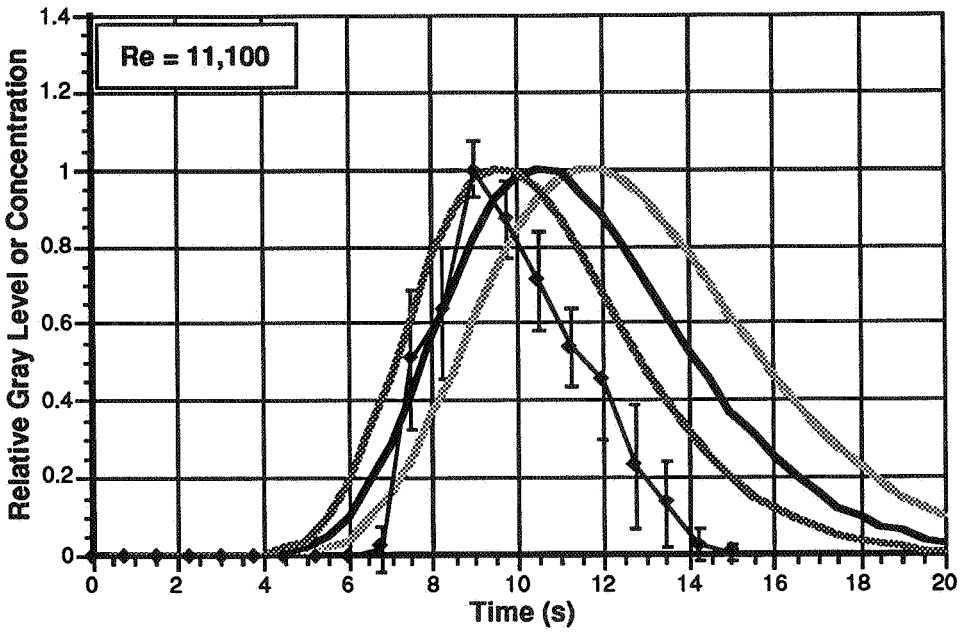

Figure 5 Comparison of measured mean gray level and predicted aerosol concentration time histories of a passing tracer pulse in a 0.30m diameter duct under conditions of transitional flow with a Reynolds number of 11,100.

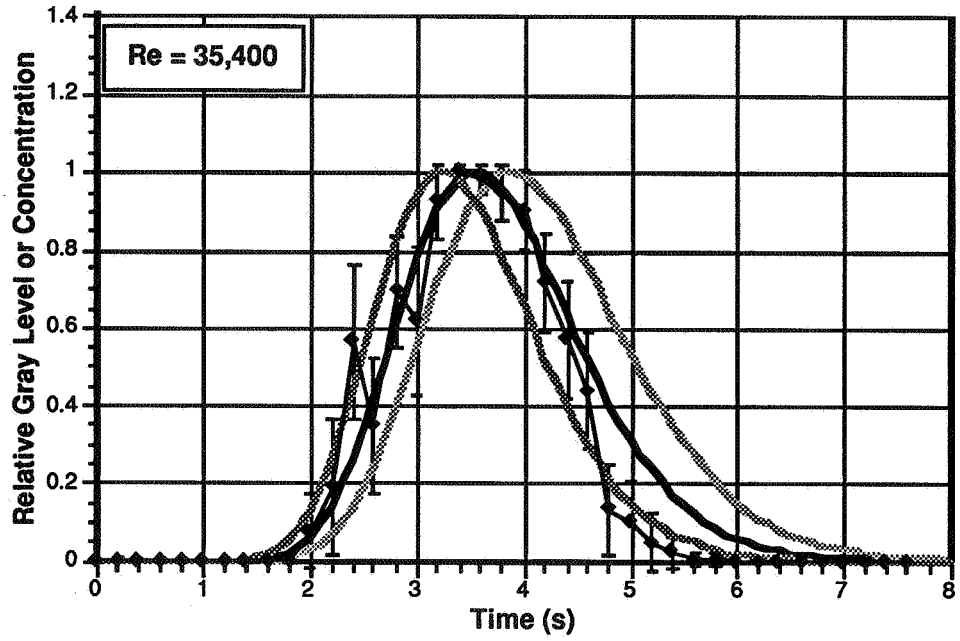

Figure 6 Comparison of measured mean gray level and predicted aerosol concentration time histories of a passing tracer pulse in a 0.30m diameter duct under conditions of turbulent flow with a Reynolds number of 35,400.

The high flow test, Figure 6 with Re = 35,400, was anticipated to present the greatest challenge to the proposed measurement system yet the results show a closer correspondence between predicted and measured dispersal than the lower flow tests even though images were captured at the rate of five per second – a data acquisition rate that should be more than sufficient for most room air distribution studies. These results are, however, consistent with theoretical expectations. That is to say, the correspondence between predicted (molecular) dispersal and measured (particle) dispersal is greatest for fully developed turbulent conditions (i.e., Re > 10,000) while at lower flow rates the axial dispersal of the Rosco fog, having a large Schmidt number, is greater than that of molecular species, hence the tracer pulses measured at the duct centerline arrived earlier than the predicted (molecular) pulses. Captured images revealed the presence of mixed laminar and medium scale turbulence providing a direct indication of transitional flow.

Somewhat surprisingly, then, these tests provided a means to evaluate the similarity of aerosol and molecular dispersal rather than challenging the acquisition rate of our equipment. The results, while not conclusive, indicate that similarity may not be realized under conditions of laminar or, even, transitional flow.

6. Conclusion

A method to measure airborne concentration distributions of an aerosol tracer over arbitrarily positioned two-dimensional planes of near-room size dimensions using laser light sheet illumination and digital image acquisition and processing techniques has been described. Technical considerations concerning the relationship between captured images and aerosol concentration and the similarity between the dispersal of the chosen aerosol tracer and molecular species dispersal have been reviewed and tests to evaluate the spatial and temporal resolution, accuracy, and repeatability of the method were discussed.

Test results presented in this paper indicate that the proposed method, using field portable, safe, and relatively inexpensive equipment, can resolve the spatial and temporal details of tracer dispersal in rooms, although similarity with molecular dispersal may not be realized for all conditions of flow. Specifically, turbulent conditions will tend to assure similarity providing aerosol settling is avoided and the aerosol tracer is seeded at sufficiently low concentrations to minimize time changes due to agglomeration, and to avoid cloud settling of injected tracer. These provisions may be realized for aerosol tracers with particle size distributions well below 10 μm by maintaining aerosol tracer concentrations below approximately 10^5 to 10^6 particles/cm^3. Similarity may not be realized under conditions of laminar or transitional flow.

Aerosol concentration may be expected to be linearly correlated to scattered light if the aerosol tracer is seeded at sufficiently low concentrations to lead to conditions of single, independent scattering and to minimize particle size changes due to agglomeration. Fortuitously, these objectives may be realized using the criteria above.

The low concentration levels demanded, however, pushed the acquisition system used in the current study to its practical limits of detectability for relatively small fields of illumination of approximately one meter square. Furthermore, due to the limited, 8-bit, dynamic range of the image acquisition system used it proved difficult to capture images that were not either clipped due to intensity saturation at the upper-end or contained pixel data that fell below the detectable limit of the system at the lower-end of the range. A next generation system should take advantage of video acquisition systems that are now available that provide greater dynamic range (i.e., 12 to 24-bit) and greater low-light sensitivity with reduced noise characteristics (e.g., cooled CCD cameras). Alternative scanning systems and, possibly, light sources will be considered in future investigations to reduce system costs.

Acknowledgment

The research reported in this paper was supported with a generous grant from the Shimizu Corporation of Japan.

References

1. RODES, C.E., R.M. KAMENS, AND R.W. WIENER, The Significance and Characteristics of the Personal Activity Cloud on Exposure Assessment Measurements for Indoor Contaminants. Indoor Air: International Journal of Indoor Air Quality and Climate, 1991. **Vol. 2**: p. pp. 123-145.
2. MURAKAMI, S. AND S. KATO, Numerical and Experimental Study on Flow and Diffusion Field in Room. Indoor Air - International Journal of Indoor Air Quality and Climate, 1991. **DRAFT.**
3. CHEN, Q., P. SUTER, AND A. MOSER, A Data Base for Assessing Indoor Airflow, Air Quality, and Draft Risk. ASHRAE Transactions, 1991. **Vol. 97**(Pt. 2).
4. WHITTLE, G.E. Evaluation of Measured and Computed Test Case Results from Annex 20, Subtask 1. in 12th AIVC Conference: Air Movement and Ventilation Control Within Buildings. 1991. Ottawa, Canada: Air Infiltration and Ventilation Centre, Coventry, Great Britain.
5. LIDDAMENT, M., Technical Note AIVC 33: A Review of Building Air Flow Simulation. 1991, Air Infiltration and Ventilation Centre:
6. PORCAR, R., J.P. PRENEL, AND G. DIEMUNSCH, An Optical Method to the Study of Instabilities in Flows, in Fluid Control and Measurement, M. Harada, Editor. 1986, Pergamaon Press: Oxford. p. 731-738.
7. MURAKAMI, S., S. KATO, AND S. AKABAYASHI, Visualization with Laser Light Sheet Applied to Internal and External Air Flows in Building Environmental Engineering, in Fluid Control and Measurement, M. Harada, Editor. 1986, Pergamaon Press: Oxford. p. 731-738.
8. SAUNDERS, D.D. AND L.D. ALBRIGHT. A Quantitative Air-mixing Visualization Technique for Two-Dimensional Flow Using Aerosol Tracers and Digital Image Analysis. in Building Systems: Room Air and Air Contaminant Distribution. 1988. University of Illinois at Urbana-Champaign: ASHRAE.
9. LONG, M.B., B.T. CHU, AND R.K. CHANG, Instantaneous Two-Dimensional Gas Concentration Measurements by Light Scattering. AIAA Journal, 1981. **Vol. 19**(No. 9): p. pp. 1151-1157.
10. ESCODA, M.C. AND M.B. LONG, Rayleigh Scattering Measurements of the Gas Field in Turbulent Jets. AIAA Journal, 1983. **Vol. 21**(No. 1): p. pp. 81-84.
11. BIRD, R.B., W.E. STEWART, AND E.N. LIGHTFOOT, Transport Phenomena. 1960, New York: John Wiley & Sons, Inc. 779 pages.
12. FRIEDLANDER, S.K., Smoke, Dust and Haze: Fundamentals of Aerosol Behavior. 1977, New York: John Wiley & Sons. 317 pages.
13. HINDS, W.C., Aerosol Technology: Properties, Behavior, and Measurment of Airborne Particles. 1982, New York: John Wiley & Sons.
14. LEVENSPIEL, O., Chemical Reaction Engineering. 1962, New York: John Wiley and Sons, Inc. 501 pages.
15. WEN, C.Y. AND L.T. FAN, Models for Flow Systems and Chemical Reactors. 1975, New York: Marcel Dekker, Inc.